https://doi.org/10.1038/s41467-023-36818-0

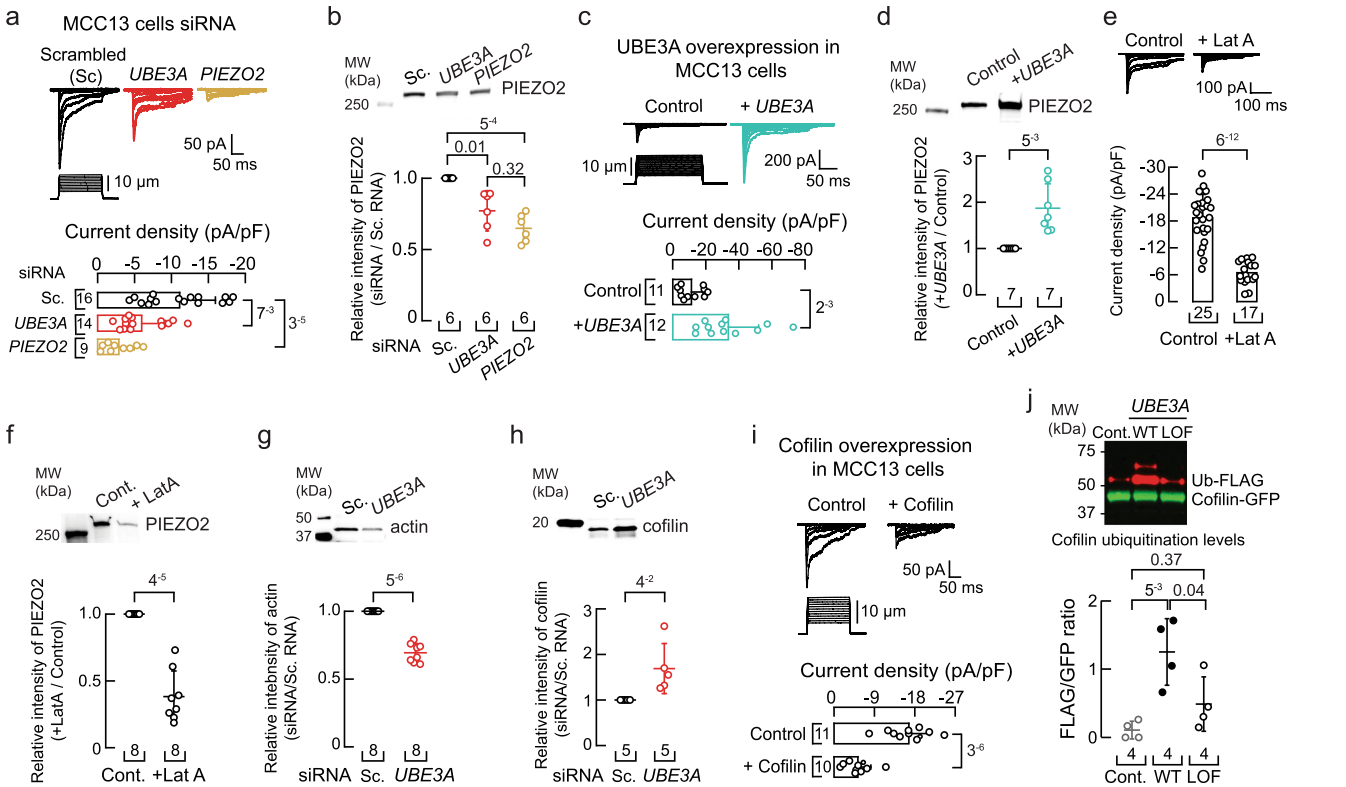

Fig. 2 | *UBE3A* knockdown increases cofilin and decreases F-actin content and PIEZO2 function. a Top, representative whole-cell patch-clamp recordings of currents elicited by mechanical stimulation (−60 mV) in MCC13 cells transfected with scrambled, *UBE3A*, or *PIEZO2* siRNAs. Bottom, current densities elicited by maximum displacement of siRNA-transfected cells. Bars are mean ± SD. Kruskal-Wallis (H = 18.76; $p = 8.4^{-5}$) and Dunn's multiple comparisons test. **b** Top, western blot (anti-PIEZO2) of the membrane fractions of MCC13 cells transfected as in (a). Bottom, mean/scatter-dot plot showing relative intensities of PIEZO2 protein normalized to PIEZO2 in the Sc. group. Lines are mean ± SD. Kruskal-Wallis (H = 12.78; $p = 0.0017$) and Dunn's multiple comparisons test. **c** Top, currents elicited by mechanical stimulation (−60 mV) in cells transfected with *UBE3A* plasmid. Bottom, current densities elicited by maximum displacement of *UBE3A* transfected cells. Bars are mean ± SD. Two-tailed unpaired *t*-test with Welch's correction ($t = 3.9$). **d** Top, western blot (anti-PIEZO2) of the membrane fractions of MCC13 cells transfected with *UBE3A* plasmid. Bottom, mean/scatter-dot plot showing relative intensities of PIEZO2 protein in *UBE3A* transfected cells normalized to PIEZO2 in the control group. Lines are mean ± SD. Two-tailed one-sample *t*-test ($t = 4.4$). **e** Top, currents elicited by mechanical stimulation (−60 mV) of latrunculin A (1 µM; 24 h)-treated MCC13 cells. Bottom, current densities elicited by maximum displacement. Bars are mean ± SD. Two-tailed unpaired *t*-test with Welch's correction ($t = 9.9$). **f** Top, western blot (anti-PIEZO2) of the membrane fractions of MCC13 cells treated as in (e). Bottom, mean/scatter-dot plot showing relative intensities of PIEZO2 protein normalized to PIEZO2 in the control group. Lines are mean ± SD. Two-tailed one-sample *t*-test ($t = -9.1$). **g** Top, western blot (anti-actin) of the cytoskeletal fractions of MCC13 transfected with scrambled (Sc.) or *UBE3A* siRNAs. Bottom, mean/scatter-dot plot showing relative intensities of actin protein normalized to actin in the Sc. group. Lines are mean ± SD. Two-tailed one-sample *t*-test ($t = -12.5$). **h** Top, western blot (anti-cofilin) of the cytosolic fractions of MCC13 transfected as in (g). Bottom, mean/scatter-dot plot showing relative intensities of cofilin protein normalized to cofilin in the Sc. group. Lines are mean ± SD. Two-tailed one-sample *t*-test ($t = 2.8$). **i** Top, currents elicited by mechanical stimulation (−60 mV) in MCC13 cells transfected with *cofilin* plasmid. Bottom, current densities elicited by maximum displacement of *cofilin* transfected cells. Bars are mean ± SD. Two-tailed unpaired *t*-test with Welch's correction ($t = 6.8$). **j** Top, western blot of pulldown GFP-tagged cofilin from HEK293T cells transfected with a control vector (Ctrl), wild-type *UBE3A* (WT), or a catalytically inactive *UBE3A* (LOF). The ubiquitinated (Ub) fraction (red) was monitored with an anti-FLAG antibody. Bottom, mean/scatter-dot plot showing Ub-FLAG/Cofilin-GFP ratios. Lines are mean ± SD. One-way ANOVA (F = 9.86; $p = 0.0054$) and Tukey multiple-comparisons test. n is denoted in each panel. Post hoc *p*-values are denoted in the corresponding panels. Source data are provided as a Source Data file.

we tested the ability of LA to enhance PIEZO2 function. To this end, we transfected *Piezo2* variant 14 (abundant in the mouse trigeminal ganglion)[51] into N2A cells lacking *Piezo1* (*Piezo1*$^{-/-}$ N2A cells)[52] to distinguish the effect of LA on PIEZO2 gating unequivocally. PIEZO2 mechanocurrents were measured after supplementing the cell media overnight with 100 µM LA. Supplementation with LA increased PIEZO2 currents twofold (−50.09 ± 19.84 pA/pF *vs.* −106.32 ± 58.9 pA/pF, mean ± SD) (Fig. 4a-b and Supplementary Fig. 4b). Overnight incubation with LA increased (~sevenfold) the plasma membrane content of this PUFA, as determined by liquid chromatography-mass spectrometry (LC-MS; Supplementary Fig. 4c). Next, we tested fatty acids of varying acyl-chain length and unsaturations to assess the chemical and structural bases whereby LA increases PIEZO2 function. We did not observe an increase in PIEZO2 activity for stearic acid (SA; C18:0), oleic acid (OA; C18:1), *ω−6* PUFAs downstream of LA [gamma linolenic acid (γLA; C18:3), dihomo gamma-linolenic acid (DγLA; C20:3), arachidonic acid (AA; C20:4), docosatetraenoic acid (DTA; 22:4)], or *ω*-3 PUFAs (αLA; C18:3 and DHA; C22:6) (Fig. 4a-b and Supplementary Fig. 4d-e). Additionally, LA slowed PIEZO2 channel inactivation in *Piezo1*$^{-/-}$ N2A cells (Fig. 4a and c). These results support that LA (C18:2), but not the other fatty acids tested, enhances PIEZO2 activity.

Similar to *Piezo1*$^{-/-}$ N2A cells, we measured a significant increase in endogenous PIEZO2 currents in MCC13 cells after overnight supplementation with LA, in a dose-dependent manner (Fig. 4d-e and Supplementary Fig. 4f). We also used an alternative supplementation protocol to add lower doses of LA for several days. Supplementing MCC13 cells with 20 µM LA each day, for five days, significantly increased PIEZO2 currents (Fig. 4d-e). These concentrations are within the range of circulating fatty acids present in the blood plasma of healthy adults[53]. Our results